

10. EXTREME CALIFORNIA RAINS DURING WINTER 2015/16: A CHANGE IN EL NIÑO TELECONNECTION?

XIAO-WEI QUAN, MARTIN HOERLING, LESLEY SMITH, JUDITH PERLWITZ, TAO ZHANG,
ANDREW HOELL, KLAUS WOLTER, AND JON EISCHEID

Failure of heavy rain in Southern California during the 2016 strong El Niño compared to flooding rains during the 1983 strong El Niño does not constitute a climate change effect.

Introduction. This is a story of two extreme events—one that was expected *but failed to occur* and the other that actually *did occur* but was not anticipated. The one that failed was extreme wetness over Southern California (SCAL) during winter 2015/16, which was predicted by seasonal forecasts. The extreme event that did occur was dryness whose considerable magnitude exacerbated one of the worst droughts on record over SCAL.

Ranked among the three strongest historical El Niño events, the 2015/16 event fueled apprehensions for flooding rains over California. Analogs were drawn from abundant winter rain during the strong El Niño events of 1982/83 and 1997/98. NOAA's winter outlook indicated a greater than 60% probability that rain totals over SCAL would be in the upper tercile of the historical distribution (www.cpc.ncep.noaa.gov/products/archives/long_lead/llarc.ind.php).

December 2015–February 2016 precipitation over SCAL was 112 mm, which ranked in the lower tercile of the historical distribution of winter precipitation since 1895 (Fig. 10.1). While not unusual from a historical perspective (Fig. ES10.1a), this dryness was an extreme event when taking account of precipitation likelihoods during strong El Niño conditions (e.g., Hoell et al. 2016). We pose the attribution question whether a transformation of El Niño teleconnections has occurred due to climate change, the effect of which may have made such an extreme dry outcome during 2015/16 more likely than during 1982/83 and 1997/98. Such a transformation could arise from changes in atmospheric circulation that mediates

trajectories of tropically forced waves (e.g., Diaz et al. 2001; Meehl and Teng 2007), or from shifts in the intensity and longitude of equatorial Pacific rainfall during El Niño events (e.g., Kug et al. 2009; Wang et al. 2015; Zhou et al. 2014). In this study, we explore whether SCAL rainfall sensitivity to a strong El Niño occurring in 2016 has changed compared to a comparably strong El Niño in 1983.

Datasets and methods. Observed monthly precipitation for 1901–2016 is from the GPCP gridded 1° resolution analysis (Schneider et al. 2013). Monthly atmospheric circulation for 1948–2016 is from the NCEP/NCAR Reanalysis (Kalnay et al. 1996). Monthly sea surface temperature (SST) and sea ice concentration (SIC) data are based on Hurrell et al. (2008).

Two ensemble suites of climate simulations are analyzed. The first is a 40-member historical transient simulation of the NCAR Community Earth System Model version 1 (CESM1; Kay et al. 2015). These “All-Forcings” simulations span 1920–2005, and use RCP8.5 for 2006–2100. The second is a 20-member ensemble of atmospheric model simulations (AMIP) generated from the atmospheric component of CESM1, named Community Atmospheric Model version 5 (CAM5; Neale et al. 2012). In these AMIP-style experiments spanning 1871–2016, observed time evolving lower boundary conditions (SSTs and SIC) are prescribed globally, while time varying external radiative forcings identical to those used in CESM1 are also specified. The atmospheric model uses horizontal resolution of $0.94^\circ \times 1.25^\circ$ and 30 vertical levels for all simulations.

While the historical AMIP ensemble size is 20-members, the ensemble size was increased to 50 members for the strong El Niño cases of 1982/83 and 2015/16. A parallel set of 50-member AMIP-style runs were conducted for these two strong El Niño events in which SST forcing over an El Niño-core region (15°N – 15°S , 175°E –South America) only was specified, while

AFFILIATIONS: QUAN, SMITH, PERLWITZ, ZHANG, WOLTER, AND EISCHEID—University of Colorado, Cooperative Institute for Research in Environmental Sciences, and NOAA Earth System Research Laboratory, Boulder, Colorado; HOERLING AND HOELL—NOAA Earth System Research Laboratory, Boulder, Colorado
DOI:10.1175/BAMS-D-17-0118.1

A supplement to this article is available online (10.1175/BAMS-D-17-0118.2)

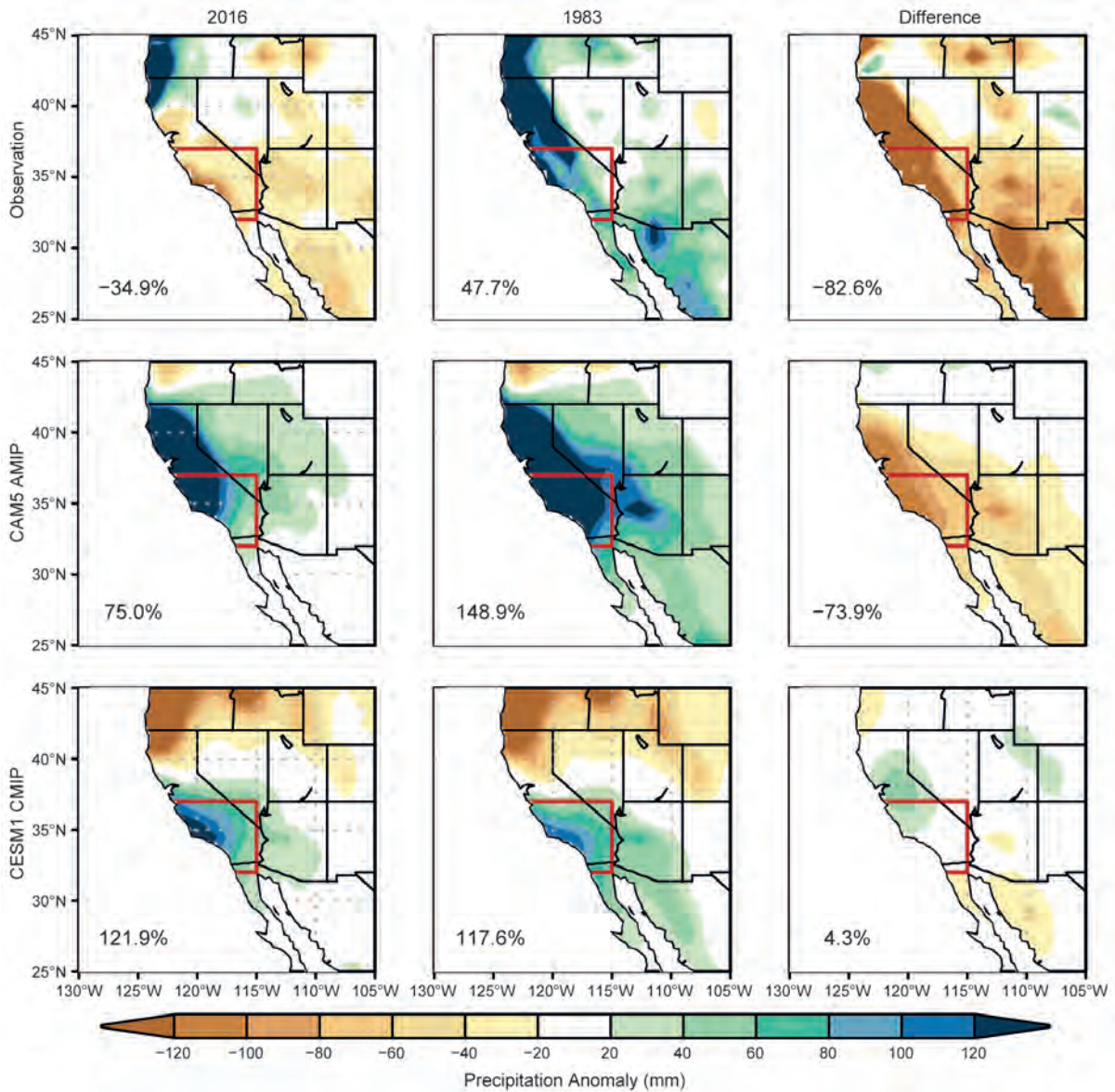


FIG. 10.1. Rows: Dec–Feb (DJF) total precipitation anomalies (mm) in observation (top), CAM5 AMIP (middle), and CESM1 (bottom) simulations. Shadings indicate difference between DJF of 2015/16 (left column), 1982/83 (middle column) and 1981–2010 climatological mean. Differences between the two strong El Niño winters are shown in right-side panels. Percentage values in each panel indicate departure of area mean of DJF total relative to observed and simulated 1981–2010 climatology of area mean, respectively. Red region denotes SCAL domain used for area averaging.

climatological SSTs were specified over the remaining world oceans. These experiments address how differences in the “flavor of El Niño” alone affected SCAL precipitation in 2016 versus 1983. Further, we address how SSTs over the “rest-of-the-world” affected SCAL precipitation by first calculating differences between the globally forced runs and the El Niño core-region runs, and then comparing these residual estimates for 2016 and 1983.

To test the effect of climate change on the response to strong El Niño, we construct composites of strong

El Niño events occurring around 1983 and 2016 by subsampling the 40-member CESM1 ensemble. Hurrell et al. (2013) demonstrate that the CESM1 realistically simulates the magnitude of the observed rise in global surface temperature during recent decades. Using a 15-year period centered in 1983 or 2016, we select all December–February warm events that exceed 1.5 times the standard deviation of the model’s Niño3.4 SST variability (1981–2010 reference). This yields strong El Niño composites having about 30–40 members for each period. Our results are robust to

an alternate method in which El Niño occurrences are calculated relative to each 15-year climatology rather than from the single 1981–2010 climatology.

Results. a. Observations. Across all regions of California, less precipitation fell during winter (December–February) 2016 compared to 1983 (Fig. 10.1, top row). For SCAL (Fig. 10.1, red outline), 2016 precipitation was 35% below the 1981–2010 mean, compared to 48% above the mean in 1983. Owing to the positive skew of SCAL climatological winter rainfall, the 2016 total was only 22% below the climatological median. It was thus not particularly extreme when assessed in an unconditional framework. However, winter rainfall statistics derived from the CAM5 AMIP simulations indicate that the observed dryness was an extreme event when conditioned upon the particular global boundary forcing of strong El Niño (Fig. ES10.1b).

The immediate cause for the drastic distinction in SCAL rainfall between 2016 and 1983 is the difference in North Pacific atmospheric circulations. Both winters exhibit features of the well-known canonical El Niño teleconnection pattern (e.g., Horel and Wallace 1981). A key distinction, however, is that the North Pacific 200-hPa negative height anomaly is weaker and shifted farther north into the Gulf of Alaska during 2016 (Fig. 10.2, top row). The circulation difference between those two winters (Fig. 10.2, top right) consists of an anticyclonic anomaly across the central North Pacific which reduced the frequency of storms over SCAL during 2016.

b. Atmospheric model simulations. The ensemble mean of CAM5 experiments indicates a SST-forced wet signal over SCAL in 2016 (Fig. 10.1, middle row), consistent with aforementioned forecast guidance. The dryness in 2016 was therefore unlikely due to boundary forcing.



FIG. 10.2. As in Fig. 10.1, but for the 200-hPa geopotential height anomalies (gpm). Contour interval is 15 m for left and middle columns, and 10 m for right column. High and low anomaly centers are denoted by H and L, respectively. Colored shadings indicate SST anomalies ($^{\circ}\text{C}$).

The magnitude of the CAM5 wet signal was diminished in 2016 when compared to 1983, however. Note especially that the simulated difference in ensemble mean California precipitation between these two winters is remarkably similar to the difference in observations. Also, comparison of the model probability density function (PDF) of SCAL precipitation in 2016 versus 1983 (Fig. ES10.1b) indicates increased likelihood for dryness in 2016; the two distributions are significantly different at the 5% level according to a Kolmogorov–Smirnov test. Nonetheless, the magnitude of observed dryness was a low probability within both ensembles.

The dynamical basis for this weaker SCAL wet signal in CAM5 is a weakened and northward displaced North Pacific low pressure in the model’s circulation pattern during 2016 (Fig. 10.2, middle row). The

model, whose El Niño driven upper tropospheric wave train agrees well with observations (Fig. 10.2, top and middle rows), indicates that upper tropospheric heights are higher across the entire Pacific basin in 2016 compared to 1983. Importantly for SCAL rainfall, differences between the height patterns of the two events consist of an anomalous anticyclonic circulation across the mid-Pacific basin which steers storms northward in 2016 relative to 1983.

Results from the El Niño core-region experiments confirm that distinct El Niño flavors (e.g., stronger far east Pacific SST warmth in 1983 but stronger central Pacific SST warmth in 2016) did not cause the Pacific–North American differences in the fully forced CAM5 simulations. Rather, the principal climate sensitivity distinguishing these two strong El Niño winters arises from the rest-of-the-world boundary conditions. In 2016 relative to 1983, these drive widespread increases in Pacific basin heights whose main feature is an anticyclonic circulation across the mid-Pacific basin (Fig. ES10.2, bottom right).

c. Coupled model simulations. To understand the AMIP results in the context of climate change, we compare CESM1 strong El Niño impacts on western U.S. precipitation for 2016 and 1983 (Fig. 10.1, bottom row). No statistically significant difference in their El Niño-related composite rainfall occurs over SCAL, even though El Niño events circa 2016 are immersed in a warmer ocean. Consistent with a warmer ocean, CESM1 indicates that climate change increases upper level heights across the entire Pacific basin (Fig. 10.2, bottom row). Importantly, however, these height increases are relatively uniform across the Pacific; there is thus no meaningful shift in the model’s El Niño-related teleconnection and hence little change in the SCAL winter precipitation. The PDF of CESM1 SCAL winter precipitation for El Niño events circa 2016 versus 1983 are statistically indistinguishable according to a Kolmogorov–Smirnov test (Fig. ES10.1c).

Conclusion. Based on transient coupled climate simulations, no transformation of El Niño teleconnections has occurred since 1983 that would materially alter the remote sensitivity of Southern California precipitation to strong El Niño forcing. Both composites of strong El Niño in CESM1 experiments circa 1983 versus 2016 show wet signals over SCAL, with no significant difference in the probability distributions for either extreme wet or extreme dry winters. We conclude that the failure of heavy rains in SCAL during the strong El Niño of 2016, compared to the

flooding rains of 1983, does not constitute a climate change effect.

Our analysis of atmospheric simulations does indicate, however, that the actual global boundary forcing in 2016 (especially the rest-of-the-world boundary forcing outside of the El Niño core-region) was significantly less favorable for wet SCAL in 2016 than in 1983. Additional experiments are required to better understand the nature of these rest-of-world boundary conditions that operated in 2016. More research is especially needed to reconcile those conditions with plausible modes of internal natural variability (Berg and Hall 2015; Kumar and Chen 2016).

ACKNOWLEDGMENTS. The authors thank three anonymous reviewers for thoughtful comments that help to improve the paper.

REFERENCES

- Berg, N., and A. Hall, 2015: Increased interannual precipitation extremes over California under climate change. *J. Climate*, **28**, 6324–6334, doi:10.1175/JCLI-D-14-00624.1
- Diaz, H., M. Hoerling, and J. Eischeid, 2001: ENSO variability, teleconnections, and climate change. *Int. J. Climatol.*, **21**, 1845–1862, doi:10.1002/joc.631.
- Hoell, A., and Coauthors, 2016: Does El Niño intensity matter for California precipitation? *Geophys. Res. Lett.*, **43**, 819–825, doi:10.1002/2015GL067102.
- Horel, J. D., and J. M. Wallace, 1981: Planetary-scale atmospheric phenomena associated with the Southern Oscillation. *Mon. Wea. Rev.*, **109**, 813–829.
- Hurrell, J., J. Hack, D. Shea, J. Caron, and J. Rosinski, 2008: A new sea surface temperature and sea ice boundary dataset for the Community Atmosphere Model. *J. Climate*, **21**, 5145–5153, doi:10.1175/2008JCLI2292.1.
- , and Coauthors, 2013: The Community Earth System Model: A framework for collaborative research. *Bull. Amer. Meteor. Soc.*, **94**, 1339–1360, doi:10.1175/BAMS-D-12-00121.1.
- Kalnay, E., and Coauthors, 1996: The NCEP/NCAR 40-year reanalysis project. *Bull. Amer. Meteor. Soc.*, **77**, 437–471.

- Kay, J. E., and Coauthors, 2015: The Community Earth System Model (CESM) Large Ensemble project: A community resource for studying climate change in the presence of internal climate variability. *Bull. Amer. Meteor. Soc.*, **96**, 1333–1349, doi:10.1175/BAMS-D-13-00255.1.
- Kug, J.-S., S.-Il An, Y.-G. Ham, and I.-S. Kang, 2009: Changes in El Niño and La Niña teleconnection over North Pacific-America in the global warming simulations. *Theor. Appl. Climatol.*, **100**, 275–282, doi:10.1007/s00704-009-0183-0.
- Kumar, A., and M. Chen, 2016: What is the variability in US west coast winter precipitation during strong El Niño events? *Climate Dyn.*, First online, doi:10.1007/s00382-016-3485-9.
- Meehl, G., and H. Teng, 2007: Multi-model changes in El Niño teleconnections over North America in a future warmer climate. *Climate Dyn.*, **29**, 779–790, doi:10.1007/s00382-007-0268-3.
- Neale, R. B., and Coauthors, 2012: Description of the NCAR Community Atmospheric Model (CAM5.0). NCAR Tech. Note NCAR/TN-486+STR, 289 pp. [Available online at www.cesm.ucar.edu/models/cesm1.0/cam/docs/description/cam5_desc.pdf.]
- Schneider, U., and Coauthors, 2013: GPCC's new land surface precipitation climatology based on quality-controlled in situ data and its role in quantifying the global water cycle. *Theor. Appl. Climatol.*, **115**, 15–40, doi:10.1007/s00704-013-0860-x.
- Wang, S.-Y., W.-R. Huang, H.-H. Hsu, and R. Gilles, 2015: Role of the strengthened El Niño teleconnection in the May 2015 floods over the Southern Great Plains. *Geophys. Res. Lett.*, **42**, 8140–8146, doi:10.1002/2015GL065211.
- Zhou, Z.-Q., S.-P. Xie, X.-T. Zheng, Q. Liu, and H. Wang, 2014: Global warming-induced changes in El Niño teleconnections over the North Pacific and North America. *J. Climate*, **27**, 9050–9064, doi:10.1175/JCLI-D-14-00254.1.